

# MULTIRESOLUTION SIGNAL PROCESSING OF FINANCIAL MARKET OBJECTS

Ioana Boier

NVIDIA  
iboier@nvidia.com

## ABSTRACT

Multiresolution analysis has applications across many disciplines in the study of complex systems and their dynamics. Financial markets are among the most complex entities in our environment, yet mainstream quantitative models operate at predetermined scale, rely on linear correlation measures, and struggle to recognize non-linear or causal structures. In this paper, we combine neural networks known to capture non-linear associations with a multiscale decomposition to facilitate a better understanding of financial market data substructures. Quantization keeps our decompositions calibrated to market at every scale. We illustrate our approach in the context of seven use cases.

**Index Terms**— Finance, multiresolution, VQ-VAE

## 1. INTRODUCTION

Financial markets are prototypical examples of systems exhibiting multiple scales of behavior. Micro and macro-economic factors intertwine in surreptitious ways, driving the ups and downs of investment portfolios. Signal processing (SP) techniques have been adapted from engineering to finance in search of alpha, or systematic patterns that emerge from data leading to excess returns. Their main challenge lies in dealing with the high dimensionality of the data [1]. Machine learning (ML) applied to finance uses pattern learning paradigms closely connected to traditional statistical and numerical approaches [1]. ML has its own challenges: financial data is non-stationary, noisy, and often insufficient, given the high dimensionality of the space to which it belongs.

One way to reduce dimensionality is to consider the intrinsic structure present in the data. For instance, bond yields, swap rates, inflation, and foreign exchange (FX) rates can be thought of as having 1D term-structures (e.g., zero-coupon, spot, forward, or basis curves). Similarly, volatilities implied by option prices are organized as (hyper-)surfaces in 2D or higher. These structures carry information that can help reduce complexity. A typical spot swap curve could have as many as fifty tenors. Studying the corresponding time series means working in 50D space. A  $10 \times 10$  volatility grid puts us in 100D space. Knowing that these data lie, in fact, on

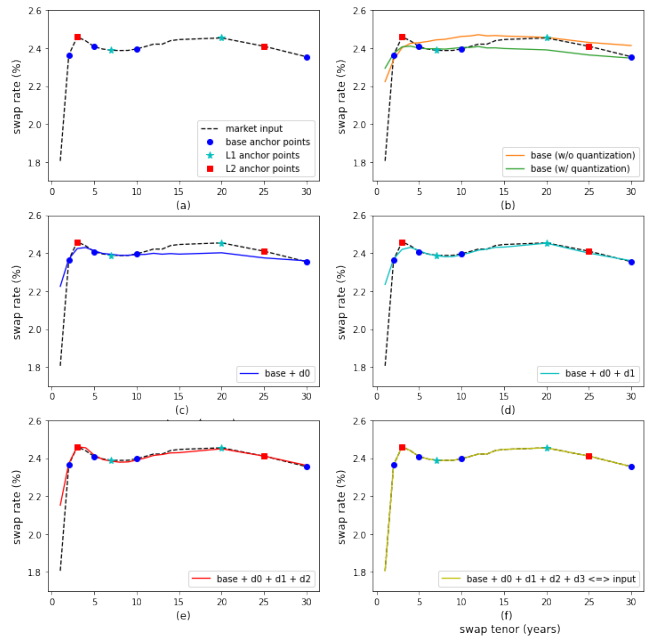


**Fig. 1.** Multiresolution decomposition of the swap curve of March 21, 2022. Anchor points are assigned to various scales by importance (e.g., market liquidity). The input curve (a) is decomposed into approximations from coarse to fine, calibrated to the anchors on each layer (base and  $L_0$  layers share the same anchors). Figures (b) through (e) illustrate the intermediate outputs from our FinQ-VAE model, while (f), reproduces the input after incorporating the final residuals.

$n$ D manifolds where  $n$  is relatively small, greatly reduces the burden of the learning task. We refer to these market data structures as *market objects* and focus on learning market behaviors from the shape and dynamics of these representations.

We propose a *multiresolution decomposition* of market objects generated with a novel architecture (FinQ-VAE) consisting of a pipeline of variational autoencoders (VAE) with latent space quantizations guided by *financially meaningful constraints*, e.g., market liquidity or trading views. Figure 1 shows a learned multiresolution decomposition of the US swap curve of March 21, 2022.

## 2. RELATED WORK

Financial data, i.e., time series of prices, are typically *non-stationary* [2]. Hence, most SP and ML approaches operate on *returns*, i.e., changes in price from one time stamp to the next. A time series of returns is typically more “stable” and likely to pass stationarity tests [3]. However, financial data also suffers from *low signal-to-noise ratios*. Hence, any signal found is likely wiped out by differencing. To quote López de Prado [4], “returns are stationary, however memoryless, and prices have memory, however they are non-stationary”.

Multiresolution methods can be traced all the way back to Fourier transforms and wavelets [5, 6, 7]. They balance signal preservation with stationarity: a base shape acts as a noise smoother, retaining an average signal level, and a hierarchy of residuals adds refinements to the base shape while exhibiting desirable statistical properties like stationarity. In finance, multiscale approaches have primarily focused on scaling along the time dimension (minute-by-minute, daily, weekly, etc.).

We propose a novel way of learning multiresolution decompositions of financially meaningful sub-structures in the data. The inspiration comes from multiresolution geometry processing techniques for fairing and interactive editing [8]. The analogy with finance lies not only in the need to disentangle or denoise a fair shape from a noisy representation, but also in the need for scenario generation through controlled movements of *key points*. In modeling physical interactions, the type of material dictates the influence of a single edit on the surrounding shape. In modeling financial scenarios, the influence of certain points on the dynamics of their neighbors is subject to financial constraints. Points on a yield curve or on a volatility surface don’t move in isolation. They are correlated to points around them. The region of influence of such move depends on the use case. Some moves have far-reaching implications, others are more localized. The nature of the deformation is also constrained by laws of arbitrage and financial plausibility.

Autoencoders with their variational and conditional flavors [9, 10, 11] have been adopted in finance mostly for single-resolution latent learning and its applications [12, 13, 14, 15, 16, 17]. We extend these ideas in two significant ways: (a) we define a new architecture of cascading VAEs to learn hierarchical decompositions of market objects and we illustrate how to leverage them in a variety of applications and (b) we introduce a quantization step [18] that takes into account financially meaningful constraints to ensure calibration to market at every scale.

## 3. FINQ-VAE

### 3.1. Modeling Background

VAEs facilitate the learning of probabilistic generative models from a set of observations in  $x \in \mathbb{R}^d$  presumed to lie on a manifold of dimension  $r \leq d$ . The loss function to be optimized during training is according to [19]:

$$\mathcal{L}(\theta, \phi, \beta; x, z) = \mathbb{E}_{q_\phi(z|x)}[\log p_\theta(x|z)] - \beta D_{KL}(\log q_\phi(z|x) || p(z))$$

With its roots in signal processing theory, *quantization* helps compress continuous sets of values to a countable or even finite number of options beyond which the variability in values makes little or no contribution to modeling. For example, images can be viewed as containing discrete objects along with a discrete set of qualifiers such as color, shape, texture. Vector-quantized VAEs (VQ-VAE) have been developed to support discrete learning [18, 20]. Market objects also contain redundant information. Moreover, like higher-level objects in images, they are, by definition, discrete collections of sub-objects with qualifiers such as steepness, curvature, skews, smiles, liquid and illiquid regions. Therefore, it makes sense to consider the benefits of quantizing their latent spaces. By default, however, VAE outputs are not faithful to specific data. In finance it is important to calibrate models to *market-observed data* or to *enforce desired constraints*. Instead of using a full-fledged VQ-VAE, we employ a simpler, non-learned quantization process that snaps encoder outputs to optimal latent locations via optimization with constraints. These dynamically quantized points are passed to the decoder to produce calibrated reconstructions which are used to compute residuals for the next layer. Consequently, our multiresolution decompositions are *calibrated to market at each scale*.

### 3.2. Problem Statement

Given a market object  $\mathcal{O}_{mkt}$ , our goal is to learn a multiresolution decomposition such that:

1. It consists of a base shape object  $\mathcal{O}_{base}$  and a number  $n + 1$  of residual layers,  $L_0, L_1, \dots, L_n$  and objects  $\delta_0, \delta_1, \dots, \delta_n$  such that  $\mathcal{O}_{mkt} = \mathcal{O}_{base} + \delta_0 + \delta_1 + \dots + \delta_n$ .
2. *Anchor points* are selected on each of the base and residual layers  $L_0, L_1, \dots, L_{n-1}$ :  $a_i^j$ , where  $i$  is the index of the anchor and  $j$  is the layer index. The selection criteria reflect financial considerations: e.g., some points are more liquid or tradeable.
3. Each intermediate reconstruction with  $j < n$  layers  $\mathcal{O}_j = \mathcal{O}_{base} + \delta_0 + \delta_1 + \dots + \delta_{j-1}$  is respectively calibrated to anchor points on  $L_0, L_1, \dots, L_{j-1}$ . The residuals in the last layer  $L_n$  are computed to recover the input market object exactly:  $\delta_n = \mathcal{O}_{mkt} - \mathcal{O}_{n-1}$ .

Figure 2 shows examples of user-defined anchors distributed according to market liquidity. We note that this technique applies to market objects of different dimensions with scattered constraints that need not be regularly spaced.

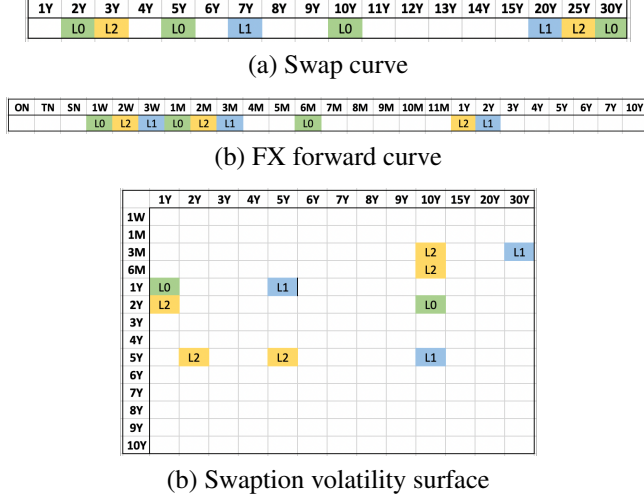


**Fig. 2.** User-specified anchor points for (a) a swap curve, (b) an FX forward curve, (c) a swaption volatility surface.

### 3.3. The FinQ-VAE Architecture

Our FinQ-VAE architecture is shown in Figure 3. Without loss of generality, we illustrate it in the context of swap curves, but the same concept applies to other types of market objects. The training inputs are market objects  $\mathcal{O}_{mkt}$  and anchors  $\mathcal{A}$  (Figure 1 (a)). Each layer is a VAE neural net, consisting of an Encoder, a Decoder, and a latent space that entails a quantization that maps encoded latent vectors into constraint-optimized vectors to be passed to the Decoder for reconstruction.

The *base layer* learns a coarse general shape (Figure 4). In this example, the  $Encoder_{base}$  takes as input the full swap curve specified by a set of  $m = 18$  swap tenors and a set of base anchor points, e.g.,  $\mathcal{A} = \{2Y, 5Y, 10Y, 30Y\}$  (Figure 2). The output of  $Encoder_{base}$  is a latent vector  $z_{base}$  in a latent space of fixed dimension. In this example we used a 3D latent space. Without quantization,  $Decoder_{base}$  maps the latent vector  $z_{base}$  into a *base* output curve  $\mathcal{O}_{base}$ , i.e., a reconstruction representing the “learned” global shape.

This representation can be likened to a PCA reconstruction using the same number of principal components. Unlike a PCA output, the VAE-generated curves are better fitted to anchors by design. We have modified the VAE loss function to include an anchor calibration term:

$$\mathcal{L}_{recon}(x, Decoder(z)) = \|x - Decoder(z)\|_2^2 + \alpha \|x|_{\mathcal{A}} - Decoder(z)|_{\mathcal{A}}\|_2^2$$

where  $\alpha \geq 0$  and the anchors  $\mathcal{A}$  serve as constraints.

While the reconstructed base curve fits the overall shape, we would like the anchor points to be fitted even better. We quantize the latent vector  $z_{base}$  to  $z_{base}^q$  via optimization:

$$z_j^q = \underset{z}{\operatorname{argmin}} \|x|_{\mathcal{A}^j} - Decoder_j(z)|_{\mathcal{A}^j}\|_2^2 \quad (1)$$

where  $j$  is the layer index. The base curve  $\mathcal{O}_{base}^q$  reconstructed from the quantized vector is shown in Figure 1 (b). Figure 5 shows curves with the same base shape before and after quantization. Given a set of artificially generated input curves passing through the same anchors in (a), the corresponding embeddings of their base shapes in 3D latent space are shown in (b): blue points are the embeddings before quantization, orange points (overlapping) are the embeddings after quantization. The base curve reconstructions without quantization are not well calibrated to the anchors as shown in (c). Reconstructions with quantization produce a well-fitted base shape in (d).

The first *residual layer* takes as input the difference object  $\delta_0 = \mathcal{O}_{mkt} - \mathcal{O}_{base}^q$  and another VAE is trained to learn the shape of  $\delta_0$  residuals. The resulting quantized residual  $\delta_0^q$  is applied to the base object  $\mathcal{O}_{base}^q$  to produce our  $L_0$  market object reconstruction:  $\mathcal{O}_0 = \mathcal{O}_{base}^q + \delta_0^q$ , see Figure 1 (c).

The second residual layer takes as input the difference object  $\delta_1 = \mathcal{O}_{mkt} - \mathcal{O}_0$  and the process is repeated. Figures 1 (d)-(e) show the reconstructions on layers 1 and 2. The final residuals  $\delta_3 = \mathcal{O}_{mkt} - \mathcal{O}_2$  and computed to recover the input  $\mathcal{O}_{mkt}$  exactly (Figure 1 (f)).

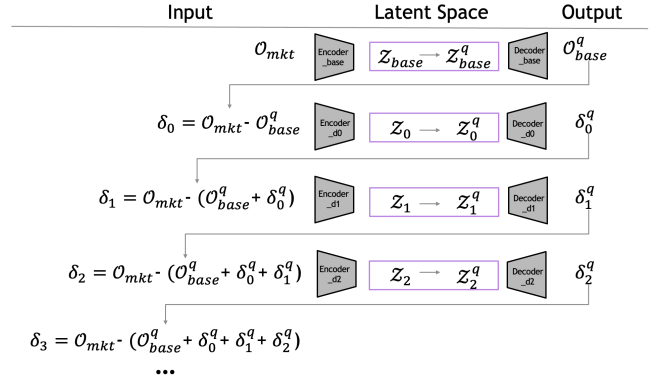


**Fig. 3.** FinQ-VAE: a pipeline of VAEs with financially quantized latent spaces is trained to learn a multiresolution decomposition of a market object into a base shape and several layers of residuals.

## 4. APPLICATIONS AND RESULTS

In this section we present seven use cases. Objects reconstructed with FinQ are not only plausible as in [21], but also calibrated to market. The choice of anchors at different scales is fully configurable. We trained two FinQ models: one on

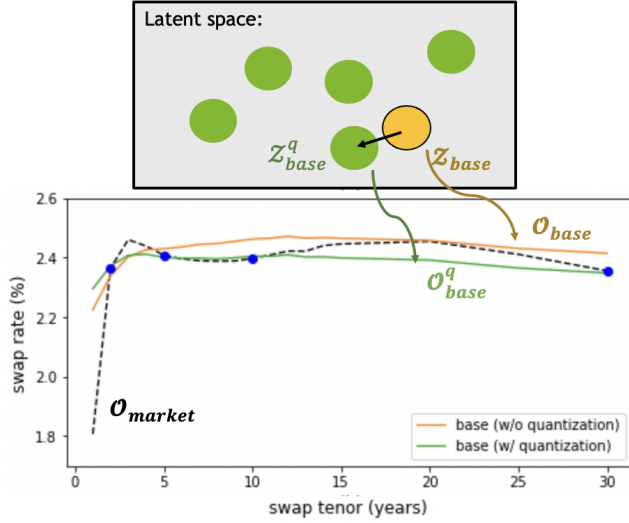


**Fig. 4.** Base curve reconstruction with constraints at anchor points (blue dots), before (orange curve) and after (green curve) quantization in latent space.

daily USD spot swap curves and one on bond curves [22] between Jan 2001 and the end of 2019. The test data period is Jan 2020 to Jul 2022. Using the magnitude of the  $L_0$  residuals as a measure of the quality of fit between the learned base curves and the actual market data around the most liquid points, we note that the model appears robust over the test data, starting in 2020. This includes the COVID-19 pandemic, the inflationary period that follows, and the start of the rate hike cycle by the US Fed, as evident in Figure 6.

### Hierarchical Factor Analysis

In contrast to PCA which typically operates on returns and ignores market levels, our multiresolution decomposition learns a global shape level on its base layer and residuals at various scales. The variational feature of the model ensures smooth navigation through latent space. The quantization feature ensures that outputs are calibrated to user-specified important points. The latter is a powerful property, as traditionally, VAEs have only been used in finance for generating “similar” data to some learned distribution that could be rather different from market-observed values. Figure 7 illustrates the hierarchy of latent spaces in our learned model.

### Scenario Generation

Standard practice in financial risk management is to shock market objects either in absolute or percentage terms. There are two main considerations: the shape of a scenario and its overall size. Traditional techniques to generate plausible scenarios revolve around historical deformations and/or artificial stresses. Unfortunately, history doesn’t often repeat itself and the generation of artificial scenarios is rather empirical: one may have a view of the movement in certain regions of the

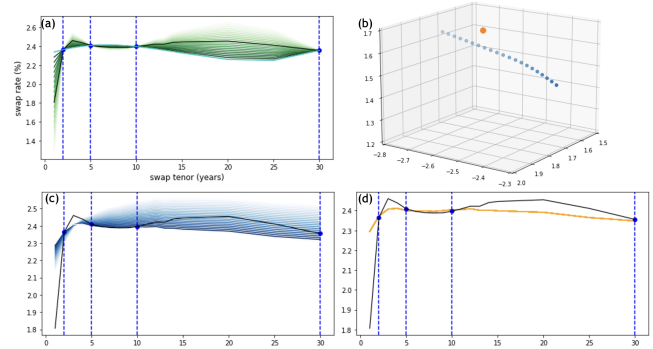


**Fig. 5.** Reconstructions with and without quantization: (a) input curves pass through the same  $L_0$  anchors; (b) embeddings of the base shapes in 3D latent space: blue points are embeddings before quantization, orange points (overlapping) are embeddings after quantization; (c) base curve reconstructions without quantization are not well calibrated to the anchors; (d) a well-fitted base shape is obtained after quantization.

market, but the dependence of the rest of the market to movements in those regions may be difficult to ascertain. PCA-based techniques are appealing because of their simplicity, however proper calibration of scenario size is challenging and global dependence on non-intuitively weighted linear combinations of points is difficult to interpret.

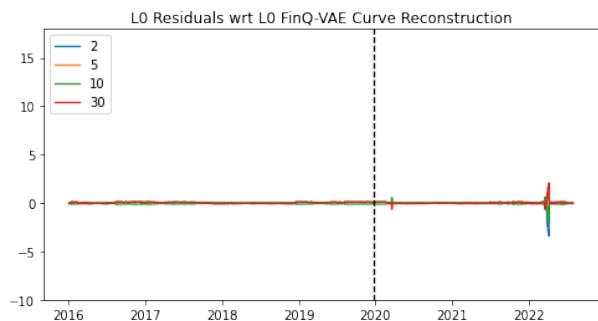
Our multiresolution framework splits responsibilities: base shapes account for market levels and are under the control of a few key drivers that are easier to intuit by human experts. Their views define anchor points and desired stresses. Dependencies that are more difficult to synthesize through human experience are generated algorithmically (Figure 9).

### Synthetic Data Generation

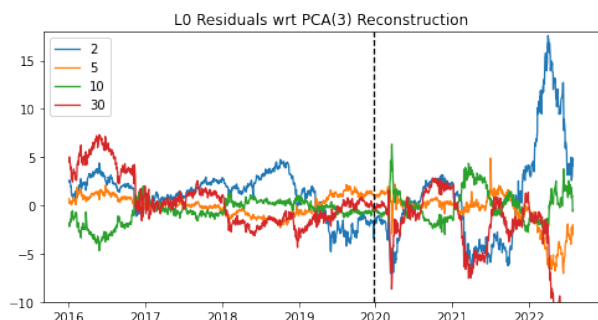
Synthetic market objects are composable in hierarchical fashion. This can be done artificially by sampling the latent spaces of the VAEs from coarse to fine, or by using historical or trader-specified moves of anchor points for the lower layers in the hierarchy and randomly sampling the higher ones. Figure 10 illustrates synthetic samples on each level.

### Nowcasting

Nowcasting is the “forecasting” of the present or the near future in the absence of complete information about the current state of the market. It has two main components: an understanding of what is already priced in the market and a view on future conditions. We allow for such views to be incorporated. For example, option portfolios require full implied volatility surfaces to price, yet option prices may not be available for all (*expiry, underlier*) pairs. The most liquid points can be used as anchors, while missing values can be sampled from the latent distributions. In the examples of Figure 9, the scenario curves are reconstructed from the known current



(a)



(b)

**Fig. 6.** (a) Liquid point residuals (2Y, 5Y, 10Y, 30Y) with respect to the  $L_0$  FinQ-VAE reconstruction are relatively small in magnitude and stable, including over the test period starting in 2020. (b) Shown comparatively are the residuals with respect to a PCA reconstruction with 3 factors.

move of a single point (scenario driver) and previous residuals. Unlike conditional models, our approach does not require training with conditional labels.

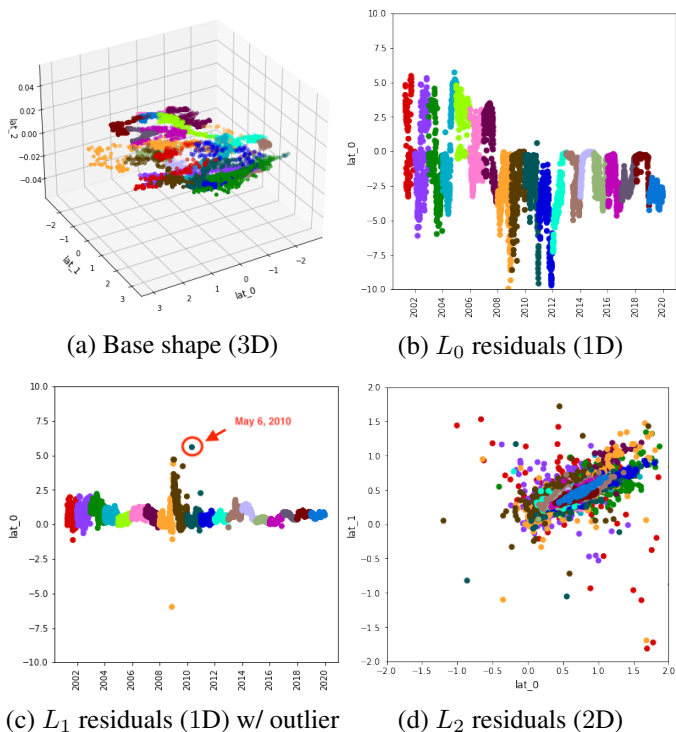
### Residuals as Signals

Residual time series could be used as signals for systematic strategies.  $\mathcal{A}_0$  anchor points should have residuals that are close to zero on  $L_0, L_1, \dots$ . If this is not the case, their deviation from zero may be used as a signal that the shapes being reconstructed are difficult to fit to the constraints. Such difficulties are harbingers of unusual market conditions.

Figure 11 depicts residuals of the 25Y swap rate with respect to the FinQ-generated  $L_0, L_1, L_2$  curves (vertical line is the boundary between train/test data). The residuals are small with respect to the  $L_2$  reconstruction since 25Y is an anchor on  $L_2$ . They are larger, but mean reverting vs. coarser reconstructions  $L_1$  and  $L_0$ , respectively.

### Relative Value Analysis

We applied FinQ to learning US Treasury bond curves. While bonds and interest rate swaps capture similar macroeconomic developments, swap curves tend to be smoother. Hence, swap



(a) Base shape (3D)

(b)  $L_0$  residuals (1D)(c)  $L_1$  residuals (1D) w/ outlier(d)  $L_2$  residuals (2D)

**Fig. 7.** Hierarchy of latent spaces (color-coded by year).

curve reconstructions could be used to identify viable swap spread trades. Figure 12 indicates that buying 30Y bonds and selling the same maturity swaps might be a good strategy.

### Outlier Detection

The variational aspect of autoencoders ensures relatively compact clusters of latent encodings. Samples that stand out from their clusters are likely to be outliers. Figure 7 (c) singles out such a point corresponding to May 6, 2010; upon closer inspection of the data (Figure 8), we notice that on this date the 20Y value seems stale, causing a non-smooth curve (the “flash crash” occurred intraday on that date, which may have contributed to noise in the end-of-day data).

## 5. CONCLUSIONS

FinQ-VAE is a novel architecture for multiresolution signal processing of market objects. Market-calibrated representations are learned using a layered approach. User-specified constraints can be incorporated at different scales to generate quantized embeddings that lead to calibrated reconstructions of market objects. To our knowledge, this is the first time multiresolution analysis is combined with quantized VAEs and applied to financial modeling in a way that accommodates constraints such as trading views, liquidity, etc. We showed that the resulting decompositions could serve in a variety of

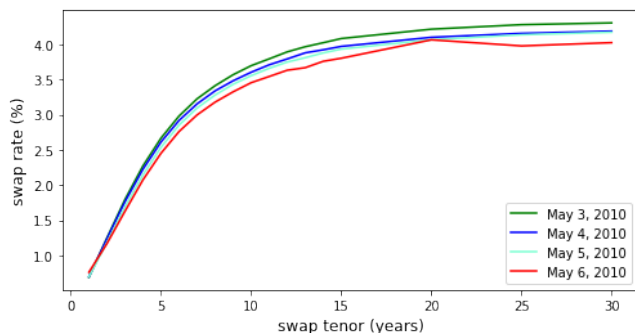


**Fig. 8.** Outlier detection: a closer inspection around May 6, 2010 reveals a curve with noise around the 20Y tenor which is an anchor on the  $L_1$  level. The resulting non-smooth curve does not correspond to the learned shape distribution, hence it appears as an outlier in the  $L_1$  latent space (see Figure 7 (c)).

use cases. Our technique applies across asset classes and different dimensionality structures.

## 6. REFERENCES

- [1] Ali N Akansu, Sanjeev R Kulkarni, and Dmitry M Malioutov, *Financial signal processing and machine learning*, John Wiley & Sons, 2016.
- [2] Rama Cont, “Empirical properties of asset returns: stylized facts and statistical issues,” *Quantitative finance*, vol. 1, no. 2, pp. 223, 2001.
- [3] Ruey S Tsay, *Analysis of financial time series*, John Wiley & sons, 2005.
- [4] Marcos López De Prado, *Advances in financial machine learning*, John Wiley & Sons, 2018.
- [5] Alfred Haar, *Zur Theorie der orthogonalen Funktionensysteme*, Georg-August Universität, Göttingen, 1909.
- [6] Ingrid Daubechies, “Time-frequency localization operators: a geometric phase space approach,” *IEEE Trans. on Infor. Theory*, vol. 34, no. 4, pp. 605–612, 1988.
- [7] Stephane G Mallat, “Multiresolution approximations and wavelet orthonormal bases of  $l^2(\mathcal{r})$ ,” *Transactions of the American mathematical society*, vol. 315, no. 1, pp. 69–87, 1989.
- [8] Ioana Boier-Martin, Remi Ronfard, and Fausto Bernardini, “Detail-preserving variational surface design with multiresolution constraints,” 2005.
- [9] David E Rumelhart, Geoffrey E Hinton, and Ronald J Williams, “Learning internal representations by error propagation,” Tech. Rep., California Univ San Diego La Jolla Inst for Cognitive Science, 1985.
- [10] Diederik P Kingma and Max Welling, “Auto-encoding variational Bayes,” *preprint arXiv:1312.6114*, 2013.
- [11] Kihyuk Sohn, Honglak Lee, and Xinchen Yan, “Learning structured output representation using deep conditional generative models,” *Advances in neural information processing systems*, vol. 28, 2015.
- [12] Alexei Kondratyev, “Learning curve dynamics with artificial neural networks,” *SSRN 3041232*, 2018.
- [13] Maxime Bergeron, Nicholas Fung, John Hull, Zissis Poulos, and Andreas Veneris, “Variational autoencoders: A hands-off approach to volatility,” *J. of Financial Data Science*, vol. 4, no. 2, pp. 125–138, 2022.
- [14] Yoshiyuki Suimon, Hiroki Sakaji, Kiyoshi Izumi, and Hiroyasu Matsushima, “Autoencoder-based three-factor model for the yield curve of japanese government bonds and a trading strategy,” *Journal of Risk and Financial Management*, vol. 13, no. 4, pp. 82, 2020.
- [15] Alexander Sokol, “Autoencoder market models for interest rates,” Tech. Rep., CompatibL Workshop, 2022.
- [16] Bryan Lim, Stefan Zohren, and Stephen Roberts, “Detecting changes in asset co-movement using the autoencoder reconstruction ratio,” *arXiv preprint arXiv:2002.02008*, 2020.
- [17] Shihao Gu, Bryan Kelly, and Dacheng Xiu, “Autoencoder asset pricing models,” *Journal of Econometrics*, vol. 222, no. 1, pp. 429–450, 2021.
- [18] Ali Razavi, Aaron Van den Oord, and Oriol Vinyals, “Generating diverse high-fidelity images with VQ-VAE-2,” *Advances in neural information processing systems*, vol. 32, 2019.
- [19] Irina Higgins, Loic Matthey, Arka Pal, Christopher Burgess, Xavier Glorot, Matthew Botvinick, Shakir Mohamed, and Alexander Lerchner, “beta-VAE: Learning basic visual concepts with a constrained variational framework,” in *Intl. Conf. on Learning Repr.*, 2017.
- [20] Aaron Van Den Oord, Oriol Vinyals, et al., “Neural discrete representation learning,” *Advances in neural information processing systems*, vol. 30, 2017.
- [21] Pierre Henry-Labordere, “Generative models for financial data,” *Available at SSRN 3408007*, 2019.
- [22] Board of Governors of the Federal Reserve System (US), “Fitted yield from FRED, Federal Reserve Bank of St. Louis,” <https://fred.stlouisfed.org/series/THREEFY5>.

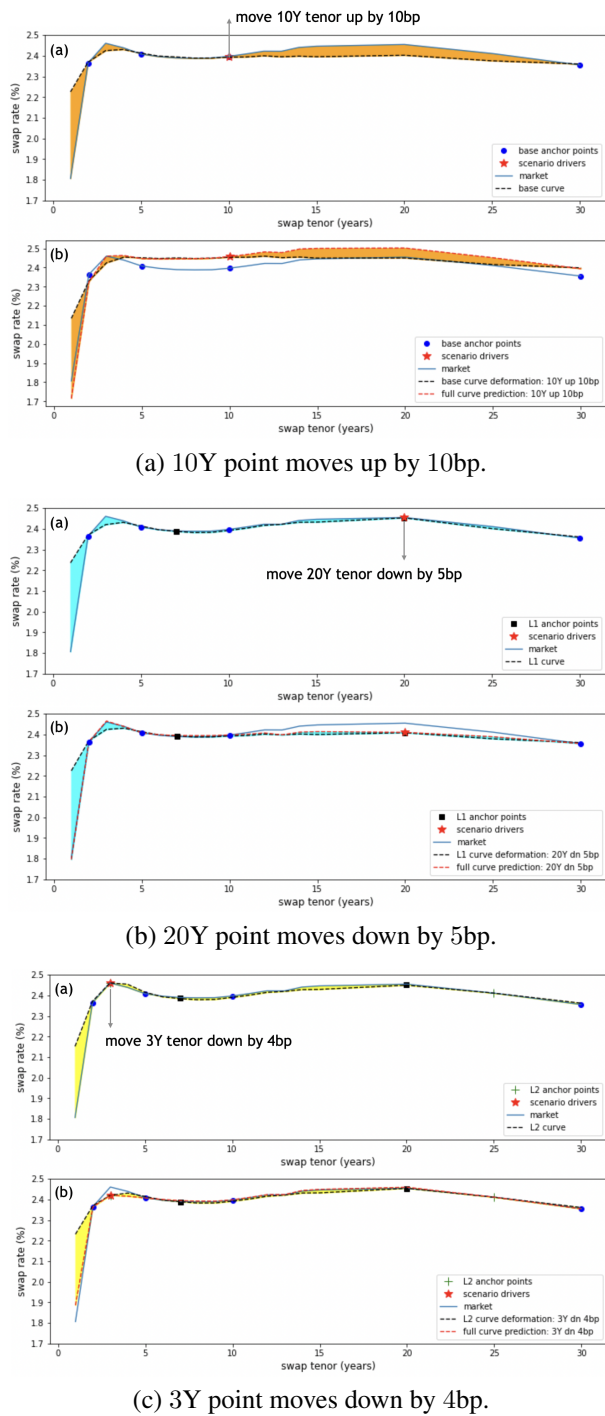


**Fig. 9.** Full curve scenarios conditional on user moves. Coarse-to-fine anchor points have global-to-local impacts.

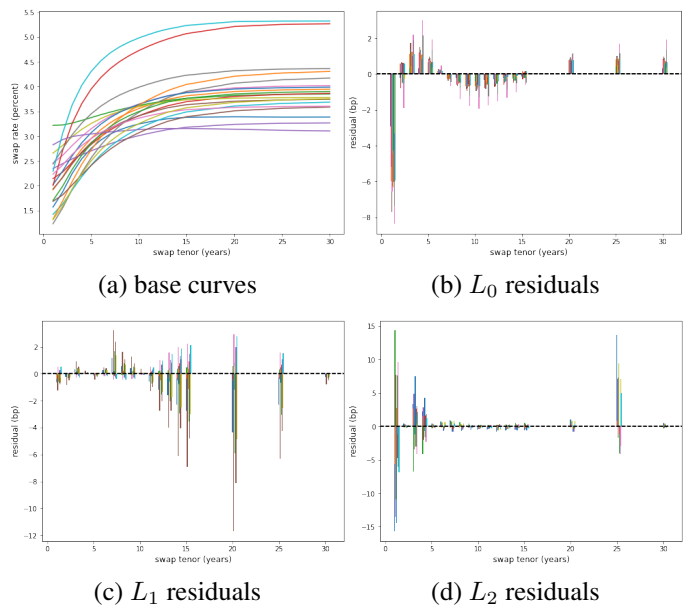


**Fig. 10.** Synthetic samples generated at various scales.

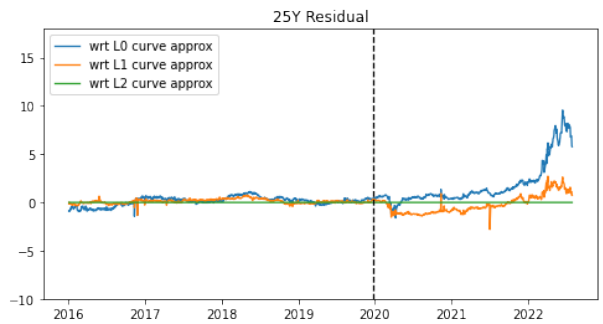


**Fig. 11.** 25Y residuals vs.  $L_0, L_1, L_2$  reconstructions.

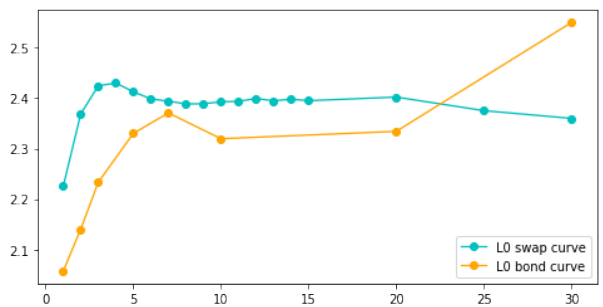


**Fig. 12.** Relative value analysis of bond yields vs. swap rates.